CHAPTER 4

Crystal Defects and Noncrystalline Structure—Imperfection

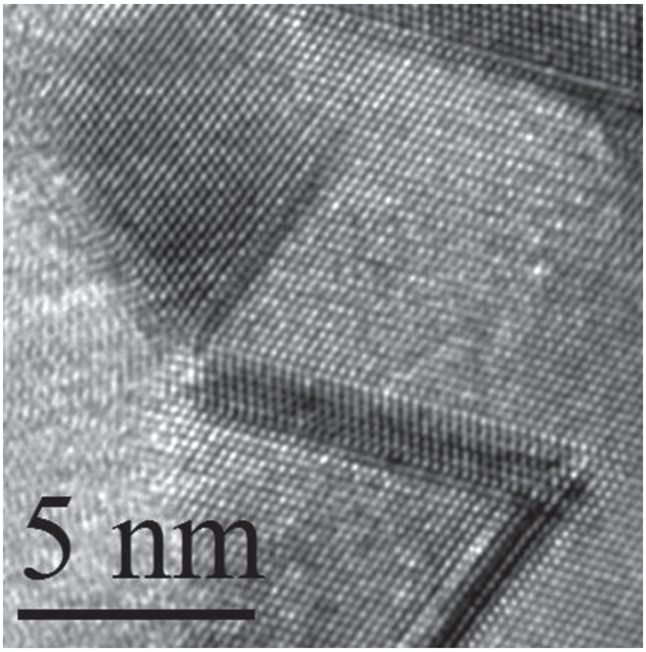

In contrast to the "perfect" structures of Chapter 3, this high-resolution transmission electron micrograph shows irregularities in the packing of atoms including the twin boundaries in the lower right-hand corner of this image of a diamond film. Such two-dimensional defects are among the topics of this chapter. (Courtesy of Klaus van Benthem, Andrew Thron, and David Horsley, University of California, Davis.)

4.1 The Solid Solution—Chemical Imperfection

It is not possible to avoid some contamination of practical materials. Even high-purity semiconductor products have some measurable level of impurity atoms. Many engineering materials contain significant amounts of several different

Shackelford, James. Introduction to Materials Science for Engineers, Global Edition, Pearson Education Limited, 2015. ProQuest Ebook Central,
http://ebookcentral.proquest.com/lib/ethz/detail.action?docID=5173617.
Created from ethz on 2020-01-08 00:01:25.

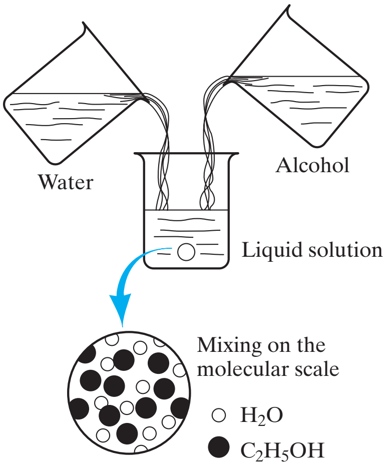

FIGURE 4.1 *Forming a liquid solution of water and alcohol. Mixing occurs on the molecular scale.*

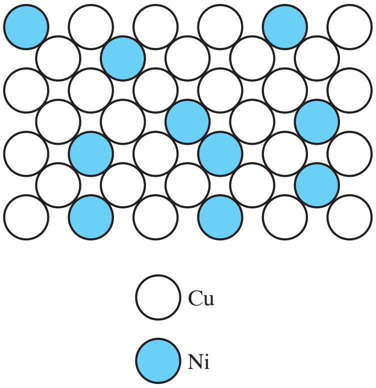

FIGURE 4.2 *Solid solution of nickel in copper shown along a* (100) *plane. This is a substitutional solid solution with nickel atoms substituting for copper atoms on fcc atom sites.*

components. Commercial metal alloys are examples. As a result, all materials that the engineer deals with on a daily basis are actually **solid solutions**. At first, the concept of a solid solution may be difficult to grasp. In fact, it is essentially equivalent to the more familiar liquid solution, such as the water–alcohol system shown in Figure 4.1. The complete solubility of alcohol in water is the result of complete molecular mixing. A similar result is seen in Figure 4.2, which shows a solid solution of copper and nickel atoms sharing the fcc crystal structure. Nickel acts as a **solute** dissolving in the copper **solvent**. This particular configuration is referred to as a **substitutional solid solution** because the nickel atoms are substituting for copper atoms on the fcc atom sites. This configuration will tend to occur when the atoms do not differ greatly in size. The water–alcohol system shown in Figure 4.1 represents two liquids completely soluble in each other in all proportions. For this complete miscibility to occur in metallic solid solutions, the two metals must be quite similar, as defined by the **Hume-Rothery*** **rules**:

1. Less than about 15% difference in atomic radii
2. The same crystal structure
3. Similar electronegativities (the ability of the atom to attract an electron)
4. The same valence

If one or more of the Hume-Rothery rules are violated, only partial solubility is possible. For example, less than 2 at % (atomic percent) silicon is soluble in aluminum. Inspection of Appendices 1 and 2 shows that Al and Si violate rules 1,

---

*William Hume-Rothery (1899–1968), British metallurgist, made major contributions to theoretical and experimental metallurgy as well as metallurgical education. His empirical rules of solid-solution formation have been a practical guide to alloy design for more than half a century.

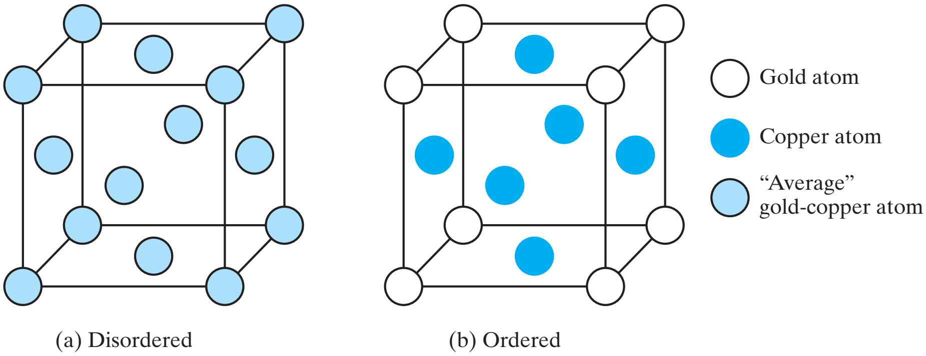

FIGURE 4.3 *Ordering of the solid solution in the* $AuCu_3$ *alloy system. (a) Above ~390°C, there is a random distribution of the Au and Cu atoms among the fcc sites. (b) Below ~390°C, the Au atoms preferentially occupy the corner positions in the unit cell, giving a simple cubic Bravais lattice. (From B. D. Cullity and S. R. Stock,* Elements of X-Ray Diffraction, *3rd ed., Prentice-Hall, Upper Saddle River, NJ, 2001.)*

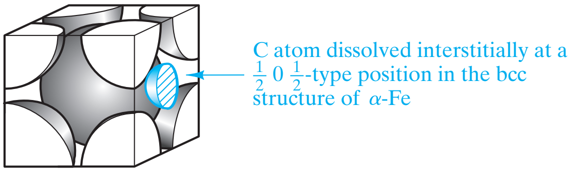

FIGURE 4.4 *Interstitial solid solution of carbon in α-iron. The carbon atom is small enough to fit with some strain in the interstice (or opening) among adjacent* Fe *atoms in this structure of importance to the steel industry. (This unit-cell structure can be compared with that shown in Figure 3.4b.)*

2, and 4. Regarding rule 3, Figure 2.21 shows that the electronegativities of Al and Si are quite different, despite their adjacent positions on the periodic table.

Figure 4.2 shows a **random solid solution**. By contrast, some systems form **ordered solid solutions**. A good example is the alloy $AuCu_3$, shown in Figure 4.3. At high temperatures (above 390°C), thermal agitation keeps a random distribution of the Au and Cu atoms among the fcc sites. Below approximately 390°C, the Cu atoms preferentially occupy the face-centered positions, and the Au atoms preferentially occupy corner positions in the unit cell. Ordering may produce a new crystal structure similar to some of the ceramic compound structures. For $AuCu_3$ at low temperatures, the compound-like structure is based on a simple cubic Bravais lattice.

When atom sizes differ greatly, substitution of the smaller atom on a crystal structure site may be energetically unstable. In this case, it is more stable for the smaller atom simply to fit into one of the spaces, or interstices, among adjacent atoms in the crystal structure. Such an **interstitial solid solution** is displayed in Figure 4.4, which shows carbon dissolved interstitially in α-Fe. This interstitial solution is a dominant phase in steels. Although more stable than a substitutional configuration of C atoms on Fe lattice sites, the interstitial structure of Figure 4.4 produces considerable strain locally to the α-Fe crystal structure, and less than 0.1 at % C is soluble in α-Fe.

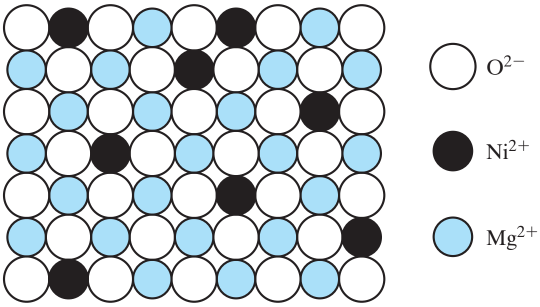

FIGURE 4.5 *Random, substitutional solid solution of* NiO *in* MgO. *The* O^{2-} *arrangement is unaffected. The substitution occurs among* Ni^{2+} *and* Mg^{2+} *ions.*

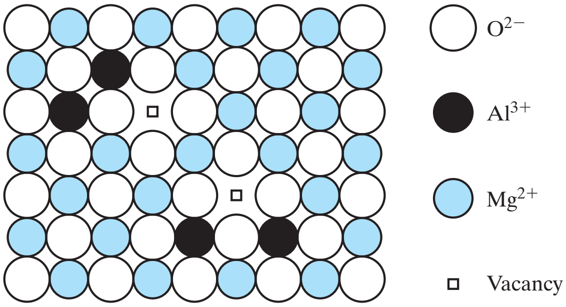

FIGURE 4.6 *A substitutional solid solution of* Al_2O_3 *in* MgO *is not as simple as the case of* NiO *in* MgO *(Figure 4.5). The requirement of charge neutrality in the overall compound permits only two* Al^{3+} *ions to fill every three* Mg^{2+} *vacant sites, leaving one* Mg^{2+} *vacancy.*

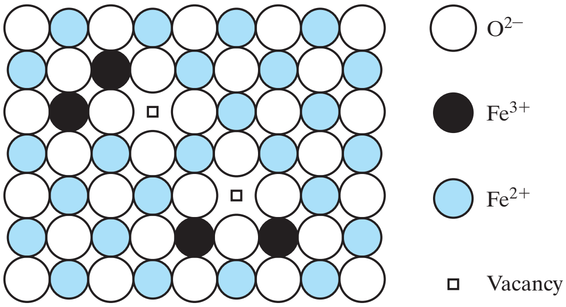

FIGURE 4.7 *Iron oxide,* $Fe_{1-x}O$ *with* $x \approx 0.05$*, is an example of a nonstoichiometric compound. Similar to the case of Figure 4.6, both* Fe^{2+} *and* Fe^{3+} *ions occupy the cation sites, with one* Fe^{2+} *vacancy occurring for every two* Fe^{3+} *ions present.*

To this point, we have looked at solid-solution formation in which a pure metal or semiconductor solvent dissolves some solute atoms either substitutionally or interstitially. The principles of substitutional solid-solution formation in these elemental systems also apply to compounds. For example, Figure 4.5 shows a random, substitutional solid solution of NiO in MgO. Here, the O^{2-} arrangement is unaffected. The substitution occurs between Ni^{2+} and Mg^{2+}. The example of Figure 4.5 is a relatively simple one. In general, the charged state for ions in a compound affects the nature of the substitution. In other words, one could not indiscriminately replace all of the Ni^{2+} ions in Figure 4.5 with Al^{3+} ions. This replacement would be equivalent to forming a solid solution of Al_2O_3 in MgO, each having distinctly different formulas and crystal structures. The higher valence of Al^{3+} would give a net positive charge to the oxide compound, creating a highly unstable condition. As a result, an additional ground rule in forming compound solid solutions is the maintenance of charge neutrality.

Figure 4.6 shows how charge neutrality is maintained in a dilute solution of Al^{3+} in MgO by having only two Al^{3+} ions fill every three Mg^{2+} sites, which leaves one Mg^{2+} site vacancy for each two Al^{3+} substitutions. This type of vacancy and several other point defects will be discussed further in Section 4.2. This example of a defect compound suggests the possibility of an even more subtle type of solid solution. Figure 4.7 shows a **nonstoichiometric compound**, $Fe_{1-x}O$, in which x is ~ 0.05. An ideally stoichiometric FeO would be identical to MgO with a

NaCl-type crystal structure consisting of equal numbers of Fe^{2+} and O^{2-} ions. However, ideal FeO is never found in nature due to the multivalent nature of iron. Some Fe^{3+} ions are always present. As a result, these Fe^{3+} ions play the same role in the $Fe_{1-x}O$ structure as Al^{3+} plays in the Al_2O_3 in MgO solid solution of Figure 4.6. One Fe^{2+} site vacancy is required to compensate for the presence of every two Fe^{3+} ions in order to maintain charge neutrality.

EXAMPLE 4.1

Do Cu and Ni satisfy Hume-Rothery's first rule for complete solid solubility?

SOLUTION

From Appendix 2,

$$r_{\mathrm{Cu}} = 0.128\ \mathrm{nm},$$

$$r_{\mathrm{Ni}} = 0.125\ \mathrm{nm},$$

and

$$\%\ \mathrm{difference} = \frac{(0.128 - 0.125)\mathrm{nm}}{0.128\ \mathrm{nm}} \times 100$$

$$= 2.3\%(< 15\%).$$

Therefore, yes.

In fact, all four rules are satisfied by these two neighbors from the periodic table (in agreement with the observation that they are completely soluble in all proportions).

EXAMPLE 4.2

How much "oversize" is the C atom in α-Fe? (See Figure 4.4.)

SOLUTION

By inspection of Figure 4.4, it is apparent that an ideal interstitial atom centered at $\frac{1}{2}0\frac{1}{2}$ would just touch the surface of the iron atom in the center of the unit-cell cube. The radius of such an ideal interstitial would be

$$r_{\mathrm{interstitial}} = \frac{1}{2}a - R,$$

where a is the length of the unit-cell edge, and R is the radius of an iron atom.

Remembering Figure 3.4, we note that

$$\text{length of unit} - \text{cell body diagonal} = 4R$$

$$= \sqrt{3}a,$$

or

$$a = \frac{4}{\sqrt{3}}R,$$

as given in Table 3.3. Then,

$$r_{\text{interstitial}} = \frac{1}{2}\left(\frac{4}{\sqrt{3}}R\right) - R = 0.1547\,R.$$

From Appendix 2, $R = 0.124$ nm, giving

$$r_{\text{interstitial}} = 0.1547(0.124\text{ nm}) = 0.0192\text{ nm}.$$

However, Appendix 2 gives $r_{\text{carbon}} = 0.077$ nm, or

$$\frac{r_{\text{carbon}}}{r_{\text{interstitial}}} = \frac{0.077\text{ nm}}{0.0192\text{ nm}} = 4.01.$$

Therefore, the carbon atom is roughly four times too large to fit next to the adjacent iron atoms without strain. The severe local distortion required for this accommodation leads to the low solubility of C in α-Fe (< 0.1 at %).

PRACTICE PROBLEM 4.1

Copper and nickel (which are completely soluble in each other) satisfy the first Hume-Rothery rule of solid solubility, as shown in Example 4.1. Aluminum and silicon are soluble in each other to only a limited degree. Do they satisfy the first Hume-Rothery rule?

PRACTICE PROBLEM 4.2

The interstitial site for dissolving a carbon atom in α-Fe was shown in Figure 4.4. Example 4.2 shows that a carbon atom is more than four times too large for the site and, consequently, carbon solubility in α-Fe is quite low. Consider now the case for interstitial solution of carbon in the high-temperature (fcc) structure of γ-Fe . The largest interstitial site for a carbon atom is a $\frac{1}{2}01$ type. **(a)** Sketch this interstitial solution in a manner similar to the structure shown in Figure 4.4. **(b)** Determine by how much the C atom in γ-Fe is oversize. (Note that the atomic radius for fcc iron is 0.127 nm.)

4.2 Point Defects—Zero-Dimensional Imperfections

Structural defects exist in real materials independently of chemical impurities. Imperfections associated with the crystalline point lattice are called **point defects**. Figure 4.8 illustrates the two common types of point defects associated with elemental solids: (1) The **vacancy** is simply an unoccupied atom site in the crystal structure, and (2) the interstitial, or **interstitialcy**, is an atom occupying an interstitial site not normally occupied by an atom in the perfect crystal structure or an extra atom inserted into the perfect crystal structure such that two atoms occupy positions close to a singly occupied atomic site in the perfect structure. In the preceding section, we saw how vacancies can be produced in compounds as a response to chemical impurities and nonstoichiometric compositions. Such vacancies can also occur independently of these chemical factors (e.g., by the thermal vibration of atoms in a solid above a temperature of absolute zero).

Figure 4.9 illustrates the two analogs of the vacancy and interstitialcy for compounds. The **Schottky* defect** is a pair of oppositely charged ion vacancies. This pairing is required in order to maintain local charge neutrality in the compound's crystal structure. The **Frenkel defect**[†] is a vacancy–interstitialcy combination. Most of the compound crystal structures described in Chapter 3 were too "tight" to allow Frenkel defect formation. However, the relatively open CaF_2-type structure can accommodate cation interstitials without excessive lattice strain. Defect structures in compounds can be further complicated by charging due to "electron trapping" or "electron hole trapping" at these lattice

POWERS OF 10

These atomic scale defects play a central role in the diffusion mechanisms of Chapter 5.

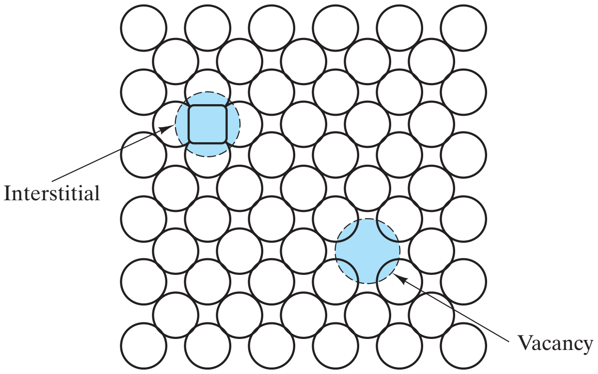

FIGURE 4.8 *Two common point defects in metal or elemental semiconductor structures are the vacancy and the interstitial.*

---

*Walter Hans Schottky (1886–1976), German physicist, was the son of a prominent mathematician. Besides identifying the *Schottky defect*, he invented the screen-grid tube (in 1915) and discovered the *Schottky effect* of thermionic emission (i.e., the current of electrons leaving a heated metal surface increases when an external electrical field is applied).

[†] Yakov Ilyich Frenkel (1894–1954), Russian physicist, made significant contributions to a wide range of areas, including solid-state physics, electrodynamics, and geophysics. Although his name is best remembered in conjunction with defect structure, he was an especially strong contributor to the understanding of ferromagnetism (a topic that is discussed in Chapter 14).

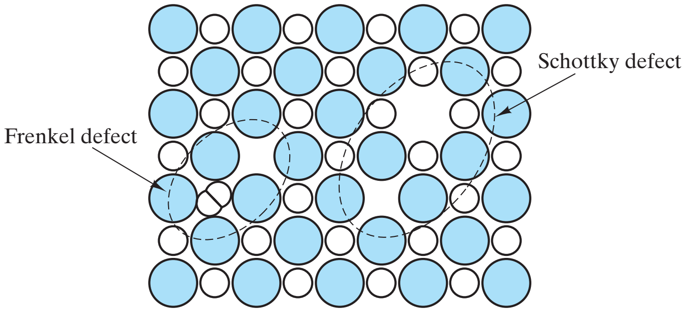

FIGURE 4.9 *Two common point defect structures in compound structures are the Schottky defect and the Frenkel defect. Note their similarity to the structures shown in Figure 4.8.*

imperfections. We shall not dwell on these more complex systems now, but can acknowledge that such defects can have important implications for optical properties (as discussed in Chapter 14).

EXAMPLE 4.3

The fraction of vacant lattice sites in a crystal is typically small. For example, the fraction of aluminum sites vacant at 400°C is 2.29×10^{-5}. Calculate the density of these sites (in units of m^{-3}).

SOLUTION

From Appendix 1, we find the density of aluminum to be 2.70 Mg/m^3 and its atomic mass to be 26.98 amu. The corresponding density of aluminum atoms is then

$$\text{at. density} = \frac{\rho}{\text{at. mass}} = \frac{2.70 \times 10^6\,\text{g/m}^3}{26.98\,\text{g}/(0.602 \times 10^{24}\,\text{atoms})}$$

$$= 6.02 \times 10^{28}\,\text{atoms} \cdot \text{m}^{-3}.$$

Then, the density of vacant sites will be

$$\text{vac. density} = 2.29 \times 10^{-5}\,\text{atom}^{-1} \times 6.02 \times 10^{28}\,\text{atoms} \cdot \text{m}^{-3}$$

$$= 1.38 \times 10^{24}\,\text{m}^{-3}.$$

PRACTICE PROBLEM 4.3

Calculate the density of vacant sites (in m^{-3}) for aluminum at 660°C (just below its melting point) where the fraction of vacant lattice sites is 8.82×10^{-4}. (See Example 4.3.)

4.3 Linear Defects, or Dislocations—One-Dimensional Imperfections

We have seen that point (zero-dimensional) defects are structural imperfections resulting from thermal agitation. **Linear defects**, which are one-dimensional, are associated primarily with mechanical deformation. Linear defects are also known as **dislocations**. An especially simple example is shown in Figure 4.10. The linear defect is commonly designated by the "inverted T" symbol (⊥), which represents the edge of an *extra half-plane of atoms.* Such a configuration lends itself to a simple quantitative designation, the **Burgers*** **vector**, **b**. This parameter is simply the displacement vector necessary to close a stepwise loop around the defect. In the perfect crystal [Figure 4.11(a)], an $m \times n$ atomic step loop closes at the starting point. In the region of a dislocation [Figure 4.11(b)], the same loop fails to close. The closure vector **(b)** represents the magnitude of the structural defect. In Chapter 6, we shall see that the magnitude of **b** for the common metal structures (bcc, fcc, and hcp) is simply the repeat distance along the highest atomic density direction (the direction in which atoms are touching).

Figure 4.10 represents a specific type of linear defect, the **edge dislocation**, so named because the defect, or *dislocation line*, runs along the edge of the extra row of atoms. For the edge dislocation, the Burgers vector is perpendicular to the dislocation line. Figure 4.12 shows a fundamentally different type of linear defect, the **screw dislocation**, which derives its name from the spiral stacking of crystal planes around the dislocation line. *For the screw dislocation, the Burgers vector is parallel to the dislocation line.* The edge and screw dislocations can be considered the pure extremes of linear defect structure. Most linear defects in actual materials will be mixed, as shown in Figure 4.13. In this general case, the **mixed dislocation** has both edge and screw character. The Burgers vector for the mixed dislocation is neither perpendicular nor parallel to the dislocation line, but instead retains a fixed orientation in space consistent with the previous definitions for

POWERS OF 10

Nanometer scale defects such as this dislocation play a central role in the plastic deformation mechanisms of Chapter 6.

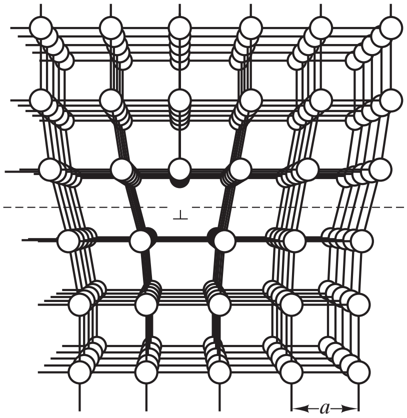

FIGURE 4.10 *Edge dislocation. The linear defect is represented by the edge of an extra half-plane of atoms. (From A. G. Guy,* Elements of Physical Metallurgy, *Addison-Wesley Publishing Co., Inc., Reading, MA, 1959.)*

---

*Johannes Martinus Burgers (1895–1981), Dutch-American fluid mechanician. Although his highly productive career centered on aerodynamics and hydrodynamics, a brief investigation of dislocation structure around 1940 has made Burgers's name one of the best known in materials science. He was the first to identify the convenience and utility of the closure vector for characterizing a dislocation.

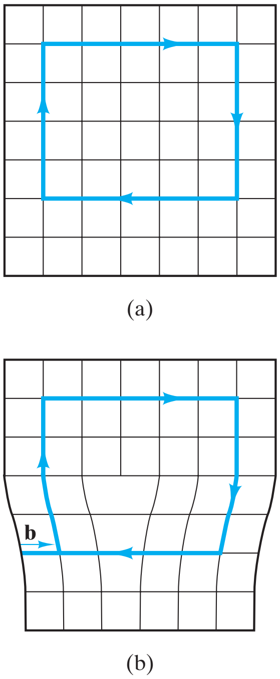

FIGURE 4.11 *Definition of the Burgers vector,* **b***, relative to an edge dislocation. (a) In the perfect crystal, an m × n atomic step loop closes at the starting point. (b) In the region of a dislocation, the same loop does not close, and the closure vector* **(b)** *represents the magnitude of the structural defect. For the edge dislocation, the Burgers vector is* perpendicular *to the dislocation line.*

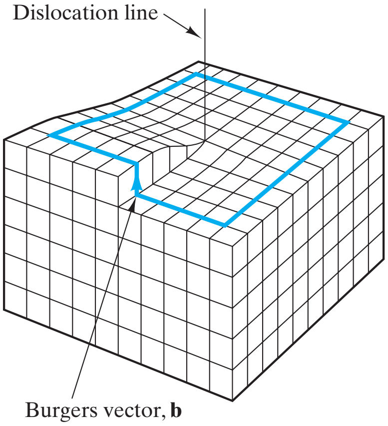

FIGURE 4.12 *Screw dislocation. The spiral stacking of crystal planes leads to the Burgers vector being parallel to the dislocation line.*

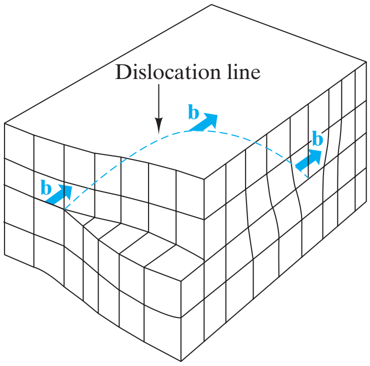

FIGURE 4.13 *Mixed dislocation. This dislocation has both edge and screw character with a single Burgers vector consistent with the pure edge and pure screw regions.*

the pure edge and pure screw regions. The local atomic structure around a mixed dislocation is difficult to visualize, but the Burgers vector provides a convenient and simple description. In compound structures, even the basic Burgers vector designation can be relatively complicated. In Chapter 6, we will see that the complexity of dislocation structures has a good deal to do with the basic mechanical behavior of the material.

EXAMPLE 4.4

Calculate the magnitude of the Burgers vector for **(a)** α-Fe and **(b)** Al.

SOLUTION

(a) As noted in the opening of this section, $|\mathbf{b}|$ is merely the repeat distance between adjacent atoms along the highest atomic density direction. For α-Fe, a bcc metal, this distance tends to be along the body diagonal of a unit cell. We saw in Figure 3.4 that Fe atoms are in contact along the body diagonal. As a result, the atomic repeat distance is

$$r = 2R_{Fe}.$$

Using Appendix 2, we can then calculate, in a simple way,

$$|\mathbf{b}| = r = 2(0.124\text{ nm}) = 0.248\text{ nm}.$$

(b) Similarly, the highest atomic density direction in fcc metals such as Al tends to be along the face diagonal of a unit cell. As shown

Shackelford, James. Introduction to Materials Science for Engineers, Global Edition, Pearson Education Limited, 2015. ProQuest Ebook Central, http://ebookcentral.proquest.com/lib/ethz/detail.action?docID=5173617.
Created from ethz on 2020-01-08 00:01:25.

in Figure 3.5, this direction is also a line of contact for atoms in an fcc structure. Again,

$$
\begin{aligned}
|\mathbf{b}| = r = 2R_{\mathrm{Al}} &= 2(0.143 \text{ nm}) \\
&= 0.286 \text{ nm}.
\end{aligned}
$$

PRACTICE PROBLEM 4.4

Calculate the magnitude of the Burgers vector for an hcp metal, Mg. (See Example 4.4.)

4.4 Planar Defects—Two-Dimensional Imperfections

Point defects and linear defects are acknowledgments that crystalline materials cannot be made flaw-free. These imperfections exist in the interior of each of these materials. But we must also consider that we are limited to a finite amount of any material and that material is contained within some boundary surface. This surface is, in itself, a disruption of the atomic-stacking arrangement of the crystal. There are various forms of **planar defects**. We shall briefly list them, beginning with the one that is the simplest geometrically.

Figure 4.14 illustrates a **twin boundary**, which separates two crystalline regions that are, structurally, mirror images of each other. This highly symmetrical discontinuity in structure can be produced by deformation (e.g., in bcc and hcp metals) and by annealing (e.g., in fcc metals).

All crystalline materials do not exhibit twin boundaries, but all must have a *surface*. A simple view of the crystalline surface is given in Figure 4.15. This surface is little more than an abrupt end to the regular atomic stacking arrangement. One should note that this schematic illustration indicates that the surface atoms are somehow different from interior (or "bulk") atoms. This is the result of different coordination numbers for the surface atoms leading to different bonding strengths and some asymmetry. A more detailed picture of atomic-scale surface

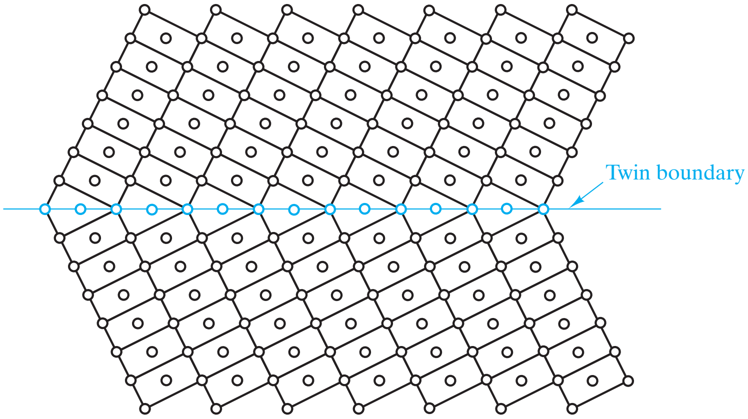

FIGURE 4.14 *A twin boundary separates two crystalline regions that are, structurally, mirror images of each other.*

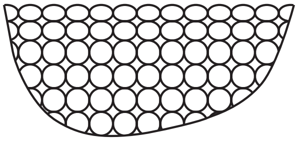

FIGURE 4.15 *Simple view of the surface of a crystalline material.*

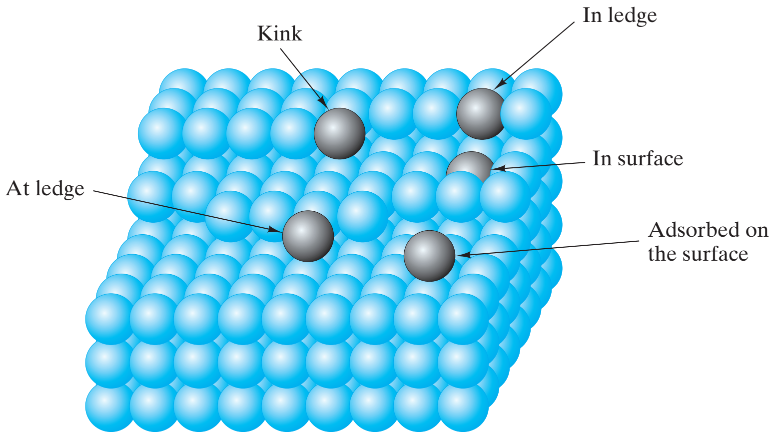

FIGURE 4.16 *A more detailed model of the elaborate ledgelike structure of the surface of a crystalline material. Various positions are indicated by shaded atoms.*

geometry is shown in Figure 4.16. This **Hirth–Pound*** **model** of a crystal surface has elaborate ledge systems rather than atomically smooth planes.

The most important planar defect for our consideration in this introductory course occurs at the **grain boundary**, the region between two adjacent single crystals, or **grains**. In the most common planar defect, the grains meeting at the boundary have different orientations. Aside from the electronics industry, most practical engineering materials are polycrystalline rather than in the form of single crystals. The predominant microstructural feature of many engineering materials is the grain structure (Figure 4.17). Many materials' properties are highly sensitive to such grain structures. What, then, is the structure of a grain boundary on the atomic scale? The answer depends greatly on the relative orientations of the adjacent grains.

Figure 4.18 illustrates an unusually simple grain boundary produced when two adjacent grains are tilted only a few degrees relative to each other. This **tilt boundary** is accommodated by a few isolated edge dislocations (see Section 4.3). Most grain boundaries involve adjacent grains at some arbitrary and rather large misorientation angle. The grain-boundary structure in this general case is considerably more complex than that shown in Figure 4.18. However, significant progress has been made in recent decades in understanding the nature of the structure of the general, high-angle grain boundary. Advances in both electron microscopy and computer modeling techniques have played primary roles in this improved understanding.

These theoretical and experimental studies of high-angle boundaries have indicated that the simple, low-angle model of Figure 4.18 serves as a useful analogy for the high-angle case. Specifically, a grain boundary between two grains at some arbitrary, high angle will tend to consist of regions of good correspondence

---

*John Price Hirth (1930–) and Guy Marshall Pound (1920–1988), American metallurgists, formulated their model of crystal surfaces in the late 1950s after careful analysis of the kinetics of vaporization.

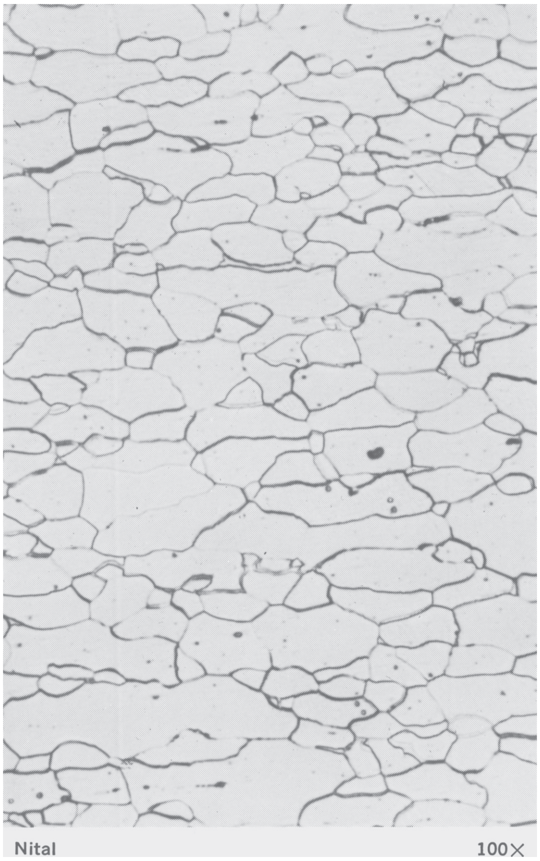

FIGURE 4.17 *Typical optical micrograph of a grain structure,* 100×. *The material is a low-carbon steel. The grain boundaries have been lightly etched with a chemical solution so that they reflect light differently from the polished grains, thereby giving a distinctive contrast. (From* Metals Handbook, *8th ed., Vol. 7:* Atlas of Microstructures of Industrial Alloys, *American Society for Metals, Metals Park, OH, 1972.)*

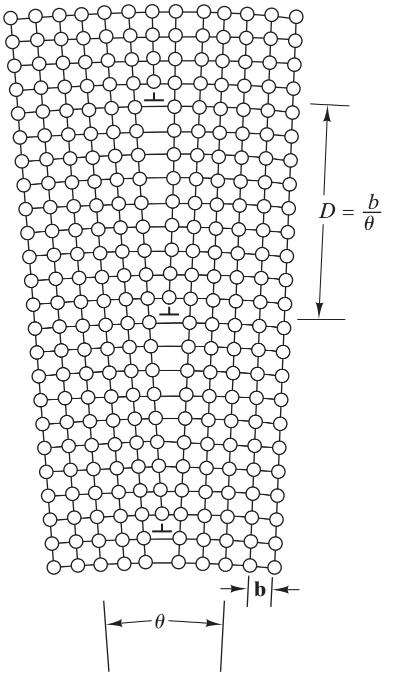

FIGURE 4.18 *Simple grain-boundary structure. This is termed a tilt boundary because it is formed when two adjacent crystalline grains are tilted relative to each other by a few degrees (θ). The resulting structure is equivalent to isolated edge dislocations separated by the distance b/θ, where b is the length of the Burgers vector,* **b**.

Micrometer-scale grain sizes such as those seen in this micrograph are typical of many common metal alloys.

separated by **grain-boundary dislocations** (GBDs), linear defects within the boundary plane. The GBD associated with high-angle boundaries tend to be *secondary* in that they have Burgers vectors different from those found in the bulk material (*primary* dislocations).

With atomic-scale structure in mind, we can return to the microstructural view of grain structures (e.g., Figure 4.17). In describing microstructures, it is useful to have a simple index of *grain size.* A frequently used parameter standardized by the American Society for Testing and Materials (ASTM) is the **grain-size number**, G, defined by

$$N = 2^{G-1}, \tag{4.1}$$

where N is the number of grains observed in an area of 1 in.^{2} (= 645 mm^2) on a photomicrograph taken at a magnification of 100 times (100×).

Although the grain-size number is a useful indicator of average grain size, it has the disadvantage of being somewhat indirect. It would be useful to obtain an average value of *grain diameter* from a microstructural section. A simple indicator is to count the number of grains intersected per unit length, n_L, of a random line drawn across a micrograph. The average grain size is roughly indicated by the inverse of n_L, corrected for the magnification, M, of the micrograph. Of course, one must consider that the random line cutting across the micrograph (in itself, a random plane cutting through the microstructure) will not tend, on average, to go along the maximum diameter of a given grain. Even for a microstructure of uniform size grains, a given planar slice (micrograph) will show various size grain sections (e.g., Figure 4.17), and a random line would indicate a range of segment lengths defined by grain-boundary intersections. In general, then, the true average grain diameter, d, is given by

$$d = \frac{C}{n_L M}, \tag{4.2}$$

where C is some constant greater than 1. Extensive analysis of the statistics of grain structures has led to various theoretical values for the constant, C. For typical microstructures, a value of $C = 1.5$ is adequate.

EXAMPLE 4.5

Calculate the separation distance of dislocations in a low-angle ($\theta = 2°$) tilt boundary in aluminum.

SOLUTION

As calculated in Example 4.4b,

$$|\mathbf{b}| = 0.286 \text{ nm}.$$

From Figure 4.18, we see that

$$\begin{aligned} D &= \frac{|\mathbf{b}|}{\theta} \\ &= \frac{0.286 \text{ nm}}{2° \times (1 \text{ rad}/57.3°)} = 8.19 \text{ nm}. \end{aligned}$$

EXAMPLE 4.6

Calculate the grain-size number, G, for a micrograph for which you measure $8.04 \dfrac{\text{grains}}{\text{in.}^2}$ at 100×.

SOLUTION

From Equation 4.1,

$$N = 2^{(G-1)}$$

or

$$
\begin{aligned}
G &= \frac{\ln N}{\ln 2} + 1 \\
&= \frac{\ln(8.04)}{\ln 2} + 1 \\
&= 4.01.
\end{aligned}
$$

PRACTICE PROBLEM 4.5

In Example 4.5, we find the separation distance between dislocations for a 2° tilt boundary in aluminum. Repeat this calculation for **(a)** $\theta = 1°$ and **(b)** $\theta = 5°$. **(c)** Plot the overall trend of D versus θ over the range $\theta = 0$ to $5°$.

PRACTICE PROBLEM 4.6

Find the grain-size number, G, for the case described in Example 4.6 if the micrograph was taken at a magnification of 300× rather than 100×.